RESEARCH PAPER

A Novel Peptide Nanomedicine Against Acute Lung Injury: GLP-1 in Phospholipid Micelles

Sok Bee Lim • Israel Rubinstein • Ruxana T. Sadikot • James E. Artwohl • Hayat Önyüksel

ABSTRACT

Purpose Treatment of acute lung injury (ALI) observed in Gram-negative sepsis represents an unmet medical need due to a high mortality rate and lack of effective treatment. Accordingly, we developed and characterized a novel nanomedicine against ALI. We showed that when human glucagon-like peptide 1(7–36) (GLP-1) self-associated with PEGylated phospholipid micelles (SSM), the resulting GLP1-SSM (hydrodynamic size, ~15 nm) exerted effective anti-inflammatory protection against lipopolysaccharide (LPS)-induced ALI in mice.

Electronic Supplementary Material The online version of this article (doi:10.1007/s11095-010-0322-4) contains supplementary material, which is available to authorized users.

S. B. Lim · H. Önyüksel
Department of Biopharmaceutical Sciences
University of Illinois at Chicago
Chicago, Illinois, USA

I. Rubinstein · R. T. Sadikot
Department of Medicine, University of Illinois at Chicago
Chicago, Illinois, USA

H. Önyüksel
Department of Bioengineering, University of Illinois at Chicago
Chicago, Illinois, USA

J. E. Artwohl
Biologic Resources Laboratory, University of Illinois at Chicago
Chicago, Illinois, USA

I. Rubinstein · R. T. Sadikot
Jesse Brown VA Medical Center
Chicago, Illinois 60612, USA

H. Önyüksel (✉)
Department of Biopharmaceutical Sciences (M/C 865)
College of Pharmacy, University of Illinois at Chicago
833 South Wood Street
Chicago, Illinois 60612-7231, USA
e-mail: hayat@uic.edu

Methods GLP1-SSM was prepared by incubating GLP-1 with SSM dispersion in saline and characterized using fluorescence spectroscopy and circular dichroism. Bioactivity was tested by in vitro cAMP induction, while in vivo anti-inflammatory effects were determined by lung neutrophil cell count, myeloperoxidase activity and pro-inflammatory cytokine levels in LPS-induced ALI mice.

Results Amphipathic GLP-1 interacted spontaneously with SSM as indicated by increased α-helicity and fluorescence emission. This association elicited increased bioactivity as determined by in vitro cAMP production. Correspondingly, subcutaneous GLP1-SSM (5–30 nmol/mouse) manifested dose-dependent decrease in lung neutrophil influx, myeloperoxidase activity and interleukin-6 in ALI mice. By contrast, GLP-1 in saline showed no significant anti-inflammatory effects against LPS-induced lung hyper-inflammatory responses.

Conclusions GLP1-SSM is a promising novel anti-inflammatory nanomedicine against ALI and should be further developed for its transition to clinics.

ABBREVIATIONS

ALI	acute lung injury
ANOVA	analysis of variance
ARDS	acute respiratory distress syndrome
BALF	bronchoalveolar lavage fluid
cAMP	cyclic adenosine monophosphate
CD	circular dichroism
CMC	critical micelle concentration
DPP-4	dipeptidyl peptidase-4
DSPE-PEG$_{2000}$	distearoyl phosphatidylethanolamine-polyethylene glycol$_{2000}$
ELISA	enzyme-linked immunosorbent assay

FBS	fetal bovine serum
GLP-1	glucagon-like peptide 1 (7–36)
GLP-1R	GLP-1 receptor
GLP1-SSM	GLP-1 peptide self-associated to SSM
HTAB	hexadecyltrimethylammonium bromide
IBMX	3-isobutyl-1-methylxanthine
IL-6	interleukin-6
LPS	lipopolysaccharide
MPO	myeloperoxidase
PEG	polyethylene glycol
RES	reticuloendothelial system
RIA	radioimmunoassay
RPM	revolutions per minute
SD	standard deviation
SSM	sterically stabilized phospholipid simple micelles
TNF-α	tumor necrosis factor-α
VIP	vasoactive intestinal peptide

INTRODUCTION

Despite recent advances in medical technology and therapeutics, acute lung injury (ALI)/acute respiratory distress syndrome (ARDS) observed in Gram-negative sepsis still represents an unmet medical need due to a high mortality rate (30–40%) and lack of effective treatment (1,2). Medical expenditure for the treatment of patients with ALI/ARDS in the intensive care unit is also highly substantial (1–3). There is, therefore, an urgent need to develop new, safe and efficacious drugs to treat this devastating disorder. To this end, we have developed and tested a novel long-acting biologic nanomedicine, human glucagon-like peptide 1(7–36) (GLP-1) self-associated with biocompatible and biodegradable PEGylated phospholipid micelles (SSM) to treat Gram-negative sepsis-induced ALI/ARDS.

Human GLP-1, a 30-amino acid amphipathic incretin hormone, has been shown to exert promising immuno-modulatory, anti-inflammatory and anti-apoptotic effects (4–6). However, human GLP-1, as with most peptides, is rapidly degraded by dipeptidyl peptidase IV (DPP-4) *in vivo*; therefore, its half-life is very short (1–2 min) (4). Accordingly, direct use of human GLP-1 as a therapeutic agent is impractical. To address this issue, several DPP-4-resistant GLP-1 analogues have been suggested (7–9). However, manufacture of these compounds is often complex and costly, more importantly, they can be associated with loss of bioactivity. Furthermore, being foreign to the body, they can cause immunogenicity and also side effects. For example, Byetta®, FDA-approved GLP-1 analogue used to treat diabetes, was shown to cause pancreatitis and acute renal failure, which are also common complications associated with ALI/ARDS (10,11).

To overcome these problems, we developed a new formulation of human GLP-1 in native form using a safe phospholipid-based nanocarrier system, sterically stabilized phospholipid micelle (SSM), and investigated its potential as a novel anti-inflammatory nanomedicine against ALI/ARDS. The nanocarrier is composed of the biocompatible and biodegradable phospholipid, 1,2-distearoyl-sn-glycero-3-phosphatidylethanolamine-N-[methoxy(polyethylene glycol)-2000 (DSPE-PEG$_{2000}$). These PEGylated phospholipid molecules self-assemble in aqueous media at lipid concentrations above their critical micelle concentration (0.5–1 μM) (12). We have previously shown that various amphipathic peptides associated spontaneously with SSM in aqueous media (13), and no chemical modification of these native peptides was required. The associated peptides are protected from enzymatic cleavage through physical shielding by the PEG palisade of SSM. Stealth property of the PEGylated phospholipid micelles would also minimize uptake by the reticuloendothelial system (RES). These effects are evidenced by the increased *in vivo* circulatory half-life of an enzyme-labile peptide, vasoactive intestinal peptide (VIP), (from 20 min to 9.5 h in mice) when associated to SSM (14). In addition, due to their particle size (~15 nm), these nanosized carriers should increase drug distribution to inflamed tissues through enhanced permeability and retention effect and abrogate renal clearance of the associated peptide (15,16). In this study, we prepared, characterized and tested, for the first time, on sepsis-induced ALI animal model this novel nanomedicine of GLP-1, an anti-inflammatory peptide, in SSM. Our results demonstrate that GLP1-SSM shows high potential to be developed as an effective anti-inflammatory therapy against lung hyper-inflammation in ALI.

MATERIALS AND METHODS

Materials

1,2-Distearoyl-sn-glycero-3-phosphatidylethanolamine-N-[methoxy(polyethylene glycol)-2000 (DSPE-PEG$_{2000}$) was purchased from LIPOID GmbH (Ludwigshafen, Germany). Human GLP-1(7–36) (GLP-1) was synthesized by Protein Research Laboratory, University of Illinois at Chicago (Chicago, IL). The peptide was HPLC purified, and the peptide purity was greater than 90% as ascertained by RP-HPLC. Synthetic exendin (9–39) was obtained from American Peptides (Sunnyvale, CA). Sterile saline (0.9% NaCl injection USP) was manufactured by Baxter Healthcare Corporation (Deerfield, IL). All other reagents were

purchased from Fisher Scientific (Ithasca, IL) or Sigma-Aldrich (St. Louis, MO).

Methods

Preparation of SSM and GLP1-SSM

GLP-1 in SSM was prepared as previously described in our laboratory (13). Briefly, weighed amount of DSPE-PEG$_{2000}$ was added to saline and vortexed for 2 min (Thermolyne Maxi Mix II) to form SSM at lipid concentrations above its critical micellar concentration (0.5–1 µM). The dispersion was then incubated at 25°C for 1 h in the dark. Thereafter, measured volume of GLP-1 stock solution (in saline) was added to SSM, and the resulting dispersion was further incubated for 2 h at 25°C in the dark.

Fluorescent Spectroscopy

The fluorescence emission spectra of GLP-1 in saline and SSM were measured using SLM Aminco 8000 Spectrofluorimeter (SLM Instruments, Rochester, NY) at room temperature (Exλ and Emλ of 275 and 340 nm, respectively). Samples were prepared with varying lipid: GLP-1 molar ratios ranging from 0 to 80:1. Peptide concentration was kept constant at 5 µM, while lipid concentration was increased from 0.0075 to 0.4 mM. The peak fluorescence emission of each sample was measured (I) and normalized against the fluorescence emission of GLP-1 in saline (I$_o$). The normalized data (I/I$_o$) were then plotted against its respective lipid: GLP-1 molar ratio using SigmaPlot® software (Systat Software, Inc., San Jose, CA). Mathematical equation of the saturation curve was generated using the curve fitting function of SigmaPlot®. The lipid: GLP-1 saturation molar ratio was determined as the lowest lipid: GLP-1 molar ratio in which the emitted fluorescence intensity of GLP1-SSM was not significantly different from the intensity measured at plateau (in the presence of excessive lipid). Given that approximately 90 lipid monomers form one SSM (17), the maximal number of GLP-1 molecules that could associate with each micelle was then calculated by the following equation:

$$\text{Number of GLP} - 1 \text{ molecules associated with one SSM} = 90/x,$$

where x is the number of lipid molecules required to associate one GLP-1 molecule at the saturation molar ratio.

Circular Dichroism

The secondary structure of GLP-1 peptide was determined using Jasco J-710 Spectropolarimeter (Jasco, Easton, MD). Spectra were scanned at room temperature in a 0.1 cm path length fused quartz under the following conditions: 190 to 260 nm at 1 nm bandwidth and 2 s response time averaged over 3 runs. Spectra were corrected for blank SSM scans and smoothed using manufacturer's Savitzky Golay algorithm.

Particle Size Analysis of GLP-1 in Saline and SSM

The aim of this experiment was to study the aggregation behavior of GLP-1 in aqueous medium (saline) and to determine if SSM could eliminate this aggregation property of GLP-1 when added to SSM dispersion. Hydrodynamic diameters (volume weighted) of GLP-1 (20 µM) in saline or SSM (5 mM DSPE-PEG$_{2000}$), and blank SSM were measured by quasi-elastic light scattering (Agilent 7030 NICOMP DLS, Agilent Technologies, Santa Clara, CA). The mean hydrodynamic particle diameters (d) in aqueous dispersions were obtained from Stokes-Einstein relation using the measured diffusion of particles in solution (η=0.933 cP, T=23°C, refractive index=1.33, scattering angle=90°). Each reported experimental result was the average of at least three d values obtained from analysis of the autocorrelation function accumulated over at least 15 min.

In Vitro Cell Culture Bioassay Studies

To evaluate the bioactivity of GLP-1 when associated with SSM, GLP1-SSM was investigated for its ability to bind and activate GLP-1 receptor (GLP-1R) in RINm5F cells via quantification of cellular cAMP production. RINm5F (ATCC# CRL-11605) cells have been shown to express GLP-1R, and the cell culture conditions employed were adapted from previous publications (18,19). The cells were seeded at a density of 2×10^5 cells per well in 6-well plate and cultured in RPMI 1640 medium (Mediatech) containing 10% fetal bovine serum (FBS) for 4 days. The culture medium was then aspirated and replaced with serum-starvation medium containing 1% FBS. After 2 h incubation, the medium was removed and replaced with 2 ml of 1 mM 3-isobutyl-1-methylxanthine (IBMX) in serum-free medium in each well. Subsequently, after 15 min incubation at 37°C, measured volume of GLP1-SSM or GLP-1 in saline was added into the respective well, and cells were treated for 10 min at 37°C. The final concentration of GLP-1 in medium was 10 nM, and the lipid: peptide molar ratio used was maintained at 15:1 for GLP1-SSM, which is around the approximate saturation molar ratio determined based on our fluorescence data. To prevent breaking up of micelles, 4 µl of 501 µM DSPE-PEG$_{2000}$ lipid solution was first pipetted into the culture medium of wells (to maintain the lipid CMC of 1 µM) into which SSM or GLP1-SSM was to be added next. At the end of the experiment, cells' lysate was collected, and

cAMP concentration was measured using enzyme-linked immunosorbent assay (ELISA) according to manufacturer's protocol (Cayman Chemical cAMP EIA). The data were normalized with the cell lysate protein content determined by Bradford assay (Bio-rad Laboratories). To investigate receptor specificity effect of GLP-1, exendin (9–39) (100 nM), a GLP-1R antagonist, was added to RINm5F cells immediately before introduction of GLP1-SSM or GLP-1 in saline. Cells were incubated and analyzed as described above.

To further investigate whether GLP1-SSM could effect similar downstream bioactivity of GLP-1R *in vitro* relative to GLP-1 in saline, stimulatory effect of GLP-1 on insulin secretion (via GLP-1R activation) by cultured rat insulinoma cells (RINm5F) was determined [18,19]. Based on previous publication [18], 2×10^5 RINm5F cells were cultured in each well of a 6 well cell culture plate (with 10% FBS containing RPMI 1640 medium) for 3 days at 37°C, 5% CO_2. Following that, the cells were washed and equilibrated for another 4 h in RPMI 1640 containing 0.5% FBS and 0.2% glucose before addition of either saline, SSM, GLP-1 in saline or GLP1-SSM (10 nM GLP-1 and a lipid: peptide molar ratio of 15:1 for GLP1-SSM). DSPE-PEG$_{2000}$ lipid solution was first added into those wells into which SSM/GLP1-SSM were to be added next to maintain lipid CMC as described above. The cells were then incubated at 37°C for 1 h. Thereafter, the culture medium was collected, centrifuged at 600 g for 5 min and assayed for insulin concentration using insulin radioimmunoassay (RIA) as per manufacturer protocol (Millipore). Radioactivity of the isotope, ^{125}I, was measured using Packard Cobra 5005 Gamma Counter (PerkinElmer, Waltham, MA).

In Vivo Anti-inflammatory Efficacy Studies Using a Murine Model of ALI

All the animal studies conducted were performed in accordance with the institutional (University of Illinois at Chicago) Animal Care Committee guidelines and to the U.S. Department of Health and Human Services Guide for the Care and Use of Laboratory Animals. To determine *in vivo* anti-inflammatory efficacy and dose response effect of GLP1-SSM, three peptide doses were tested: 5, 15 and 30 nmol (per mouse). The lipid: peptide molar ratio was kept constant at 30:1 for each peptide concentration. These peptide doses were chosen based on earlier animal study for VIP-SSM (5 nmol/mouse), on the basis that VIP belongs to the same superfamily of peptides as GLP-1 [14] and initial pilot ALI animal studies at 5 and 15 nmol of GLP-1(per mouse) which showed promising trend of anti-inflammatory efficacy. Thirty nmol of GLP1-SSM/mouse was subse-quently tested to determine potential therapeutic ceiling effect of GLP1-SSM. The ALI animal model used was modified based on earlier publications [20–22]. Using C57BL/6 male mice (8 weeks old) from Taconic Farms, Inc., lipopolysaccharide (LPS) nebulization (10 mg LPS dissolved in phosphate-buffered saline at the concentration of 1 mg/ml) was first administered via DeVilbiss disposable nebulizer (at the continuous air flow rate of 10 ft^3/h) over 1 h to induce ALI. The following control/treatment groups were evaluated ($n=6$/group): baseline control (not exposed to LPS or any treatment drug); LPS + s.c. saline; LPS + s.c. SSM; LPS + s.c. GLP-1 in saline (15 nmol of GLP-1/ mouse); LPS + s.c. GLP1-SSM at 5, 15 or 30 nmol of GLP-1/mouse; LPS + s.c. methylprednisolone (3 mg/kg). All subcutaneous injections were given in 100 µl injection volume. The animals were sacrificed 12 h after LPS nebulization [20,23]. Dose response study was only per-formed for GLP1-SSM formulation, since prior evaluation of GLP-1 in saline at 15 nmol/mouse did not show any apparent anti-inflammatory response. Since lipid: GLP-1 molar ratio was 30:1 for all GLP1-SSM formulations, the lipid doses (450 and 900 nmol of DSPE-PEG$_{2000}$/mouse) corresponding to the 2 higher peptide doses of GLP1-SSM (15 and 30 nmol of GLP-1/mouse) were tested as blank SSM controls. The lipid: peptide molar ratio was main-tained at 30:1 so that fewer GLP-1 peptide molecules would associate to each phospholipid micelle (approximate-ly 3 GLP-1 molecules per SSM). Upon *in vivo* administra-tion into mice, it was estimated that a 10-fold volume dilution would occur with our given injection volume (100 µl), leading to dissociation of some micelles (~0.2%) to maintain lipid CMC. With a lower peptide loading for each SSM, a smaller amount of GLP-1 would thus be released (and lost) as free peptide into circulation.

To assess the magnitude of lung inflammation, total and neutrophil cell counts, pro-inflammatory cytokine levels (TNF-α, IL-6) in bronchoalveolar lavage fluid (BALF), and myeloperoxidase (MPO) activity in lung tissue were measured. To quantify the total and neutrophil cell count in BALF, the collected BALF was centrifuged at 1800 rpm (Beckman GS-6R Centrifuge, Brea, CA) for 10 min at 4°C. The resulting supernatant was stored at –80°C for subsequent analysis of pro-inflammatory cytokine levels. The cell pellets were re-suspended in 0.9% normal saline and then centrifuged under the same conditions as above. The resulting cell pellets were re-suspended in 200 µl serum-free culture media (RPMI 1640), and the total cell count in each sample was determined using a grid hemocytometer under light microscope. To determine the differential (neutrophil) cell count, the remaining cell suspension was

diluted to a total volume of 1 ml or more to obtain a cell count of approximately 30,000–60,000 cells/500 µl. Cytocentrifuge slides of the cell suspension were prepared with 500 µl sample for each slide, centrifuged at 1800 rpm for 10 min (Shandon 3 Cytospin, Thermo Fisher Scientific, Waltham, MA). The slides were stained with HEMA 3 stain set, and neutrophil cell count was determined by counting 100–200 cells in cross-section under light microscope.

To determine level of pro-inflammatory cytokines (TNF-α and IL-6) in BALF, commercially available ELISA kits (R&D Systems) were used as instructed in their respective product manuals. The supernatant collected from prior centrifugation of BALF was analyzed by ELISA.

MPO activity in the extracted murine lung tissues was determined as described: weighed amount of the lung tissue was homogenized in 50 mM phosphate buffer (pH 6.0) containing 0.5% HTAB. The homogenized tissue was sonicated thrice for 15 s each using a probe sonicator (Misonix Sonicator Ultrasonic Processor XL, Qsonica, Newtown, CT) and then centrifuged at 3000 rpm (Sorvall Super T21 Centrifuge, Thermo Fisher Scientific, Waltham, MA) for 15 min at 4°C. The supernatant collected was added to the assay buffer (1:30 v/v), and absorbance (OD) was read at 460 nm at regular intervals of 30 s over 3 min in SpectraMax M5 Microplate Reader (Molecular Devices, Sunnyvale, CA). The assay buffer was composed of 50 mM phosphate buffer (pH 6.0), 0.167 mg/ml o-dianisidine hydrochloride and 0.0005% hydrogen peroxide. The MPO activity of each sample was expressed as minOD/min/g of lung tissue.

Data and Statistical Analyses

Data of all experiments were expressed as mean± standard deviation (S.D.). Any comparison between three or more groups was performed using one-way analysis of variance (ANOVA) followed by Tukey's and Fisher Least Significant Difference post-hoc analyses. For any statistical comparison between two groups, two-tailed independent Student's *t*-test was conducted. $P < 0.05$ was considered statistically significant.

RESULTS

Secondary Structure of GLP-1 in SSM

The near-UV circular dichroism (CD) spectroscopy spectra of GLP-1 (20 µM) in saline exhibited characteristic random coil secondary conformation. In the presence of SSM dispersion, the CD spectra of GLP-1 showed pronounced double minimum at approximately 208 nm and 222 nm wavelengths, which is strongly representative of a predominantly α-helical secondary conformation for GLP1-SSM (Fig. 1a).

Particle Size Analysis of GLP-1 in SSM

Nicomp® particle size analysis data of GLP-1 in saline demonstrated micron-sized aggregates with tremendously large size variance (1721.9±1285.1 nm; $n = 3$). When added to SSM, a reproducible single size peak was observed at 13.6±3.1 nm for GLP1-SSM, which was similar to the particle size of blank SSM (13.1±2.6 nm; $n = 3$) (Fig. 1b).

Drug Loading Capacity of SSM for GLP-1

The primary sequence of GLP-1 contains tryptophan and tyrosine amino acid residues that can function as its intrinsic fluorophores. Compared to GLP-1 in saline, significantly greater fluorescence emission was observed for the peptide added to SSM (Fig. 1c). This was accompanied with a blue shift in the peak fluorescence wavelength of GLP-1 in SSM (335 nm) compared to saline (350 nm), signifying a change from hydrophilic (saline) to a relatively more hydrophobic environment (micelles) (data not shown). At a constant peptide concentration (5 µM), an increasing amount of phospholipid resulted in increased fluorescence emission until the intensity leveled off to a plateau when lipid became excessive. The lowest lipid: GLP-1 molar ratio at which the emitted fluorescence became insignificantly different from the maximal fluorescence intensity at plateau was taken to be the lipid: peptide saturation molar ratio (13:1). Given that approximately 90 lipid monomers form one micelle (17), it was thereby calculated that about six GLP-1 molecules associate to each SSM at saturation.

In Vitro Bioactivity of GLP1-SSM

When added to rat insulinoma cells (RINm5F) that express GLP-1R, GLP1-SSM induced similar increase in cAMP concentration compared to GLP-1 in saline (Fig. 2a). This upregulation effect by GLP1-SSM (10 nM GLP-1) (464.4± 58.7 nM cAMP) was attenuated by co-administration of GLP-1R antagonist, exendin (9-39) (Ex, 100 nM) (213.1± 50.5 nM cAMP), indicating GLP-1R specificity for the observed effect.

Correspondingly, our data showed significantly higher insulin concentration in culture media of RINm5F cells treated with GLP-1 (10 nM) in saline (1.75±0.22-fold
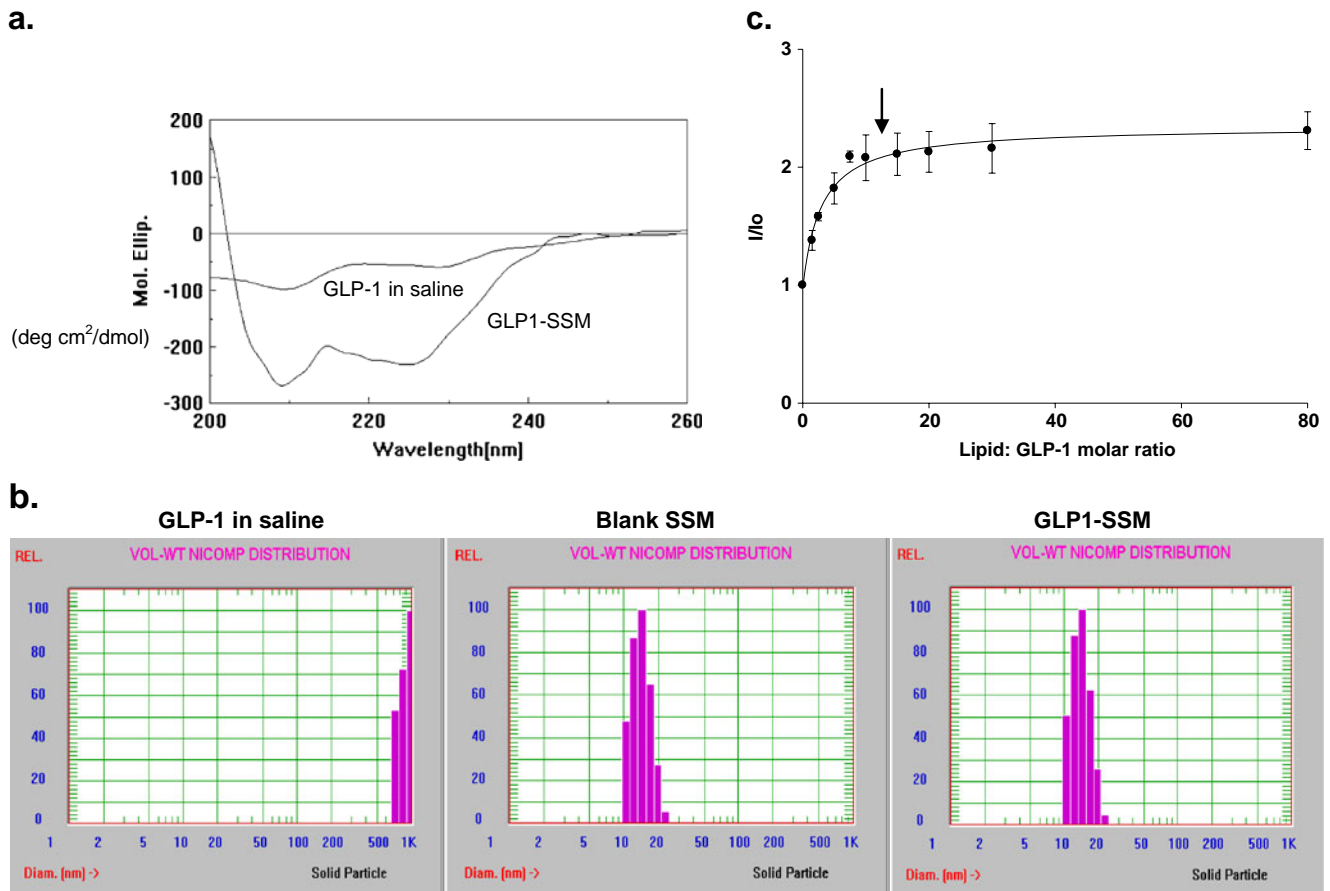
a.

c.

b.

Fig. 1 Characterization of GLP1-SSM dispersion. **a** Representative CD spectra of GLP-1 (20 μM) in saline and GLP1-SSM (5 mM DSPE-PEG$_{2000}$ lipid). **b** Representative particle size analysis data of GLP-1 (20 μM) in saline, blank SSM (5 mM DSPE-PEG$_{2000}$) and GLP1-SSM. **c** Fluorescence enhancement ratio (I/I_o) of GLP-1 (5 μM) in SSM over increasing lipid concentrations (0 - 0.4 mM). Positions of arrows indicate lipid: GLP-1 saturation molar ratio. $N = 3$ for each data point.

increase) or GLP1-SSM (1.51$\pm$0.14 fold increase), compared to control cells given saline or blank SSM, respectively ($n = 3$/group; Fig. 2b). No apparent difference was detected between GLP-1 in saline or GLP1-SSM treatment ($p > 0.05$).

In Vivo Anti-inflammatory Efficacy of GLP1-SSM Against LPS-Induced ALI

C57BL/6 mice exposed to aerosolized LPS all exhibited dramatically higher total (Fig. 3a) and differential neutrophil cell count (Fig. 3b) in BALF relative to baseline control mice not exposed to LPS nebulization. On the other hand, among those LPS-exposed mice, both the total and neutrophil (PMN) cell count were significantly lower in subcutaneous (s.c.) GLP1-SSM (15 nmol of GLP-1/mouse)-treated mice (total: 13.7$\pm$7.0$\times10^4$ cells/ml; PMN: 4.5$\pm$3.4$\times10^4$ cells/ml) compared to saline (total: 30.7$\pm$9.5$\times10^4$ cells/ml; PMN: 27.1$\pm$8.9$\times10^4$ cells/ml), SSM (total: 30.5$\pm$8.6$\times 10^4$ cells/ml; PMN: 28.3$\pm$7.5$\times10^4$ cells/ml) or GLP-1 in

saline (GLP-1) treatments (total: 43.2$\pm$17.7$\times10^4$ cells/ml; PMN: 40.0$\pm$17.4$\times10^4$ cells/ml) (each, $p < 0.05$ compared to GLP1-SSM treatment, $n = 6$/group). As with the neutrophil cell count in BALF, significantly lower myeloperoxidase (MPO) assay activity was also measured in the lung tissue of ALI mice to which GLP1-SSM (371.3$\pm$7.9 mOD/min/g of tissue) had been administered, relative to the other treatment groups (saline, 656.3$\pm$131.6 mOD/min/g of tissue; SSM, 767.6$\pm$134.3 mOD/min/g of tissue; GLP-1, 800.4$\pm$173.9 mOD/min/g of tissue) (each, $p < 0.05$ compared to GLP1-SSM treatment, $n = 6$/group) (Fig. 3c).

With respect to pro-inflammatory cytokines, increased concentration of interleukin-6 (IL-6; Fig. 4a) and tumor necrosis factor-α (TNF-α; Fig. 4b) were likewise detected in BALF of ALI mice ($p < 0.05$ relative to baseline control). Conversely, levels of these pro-inflammatory cytokines were considerably suppressed with s.c. GLP1-SSM administration (IL-6, 90.5$\pm$26.9 pg/ml; TNF-α, 61.3$\pm$24.4 pg/ml) in comparison to saline (IL-6, 212.5$\pm$83.7 pg/ml; TNF-α, 94.1$\pm$36.5 pg/ml), SSM (IL-6,
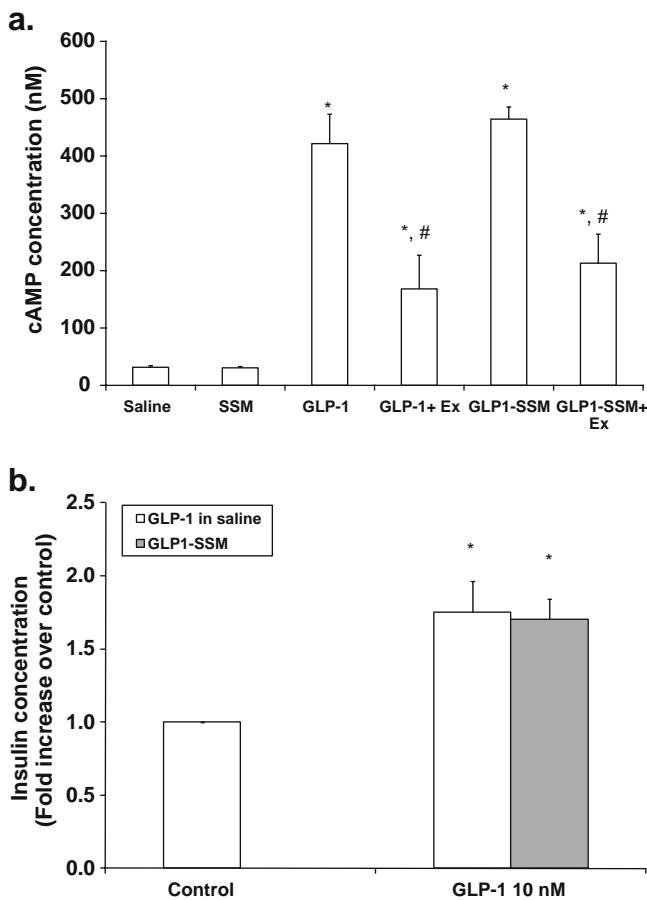
a.

b.

Fig. 2 *In vitro* bioactivity of GLP1-SSM in RINm5F insulinoma cells. **a** Normalized cAMP concentration in RINm5F cells treated with GLP-1 (10 nM) in saline or GLP1-SSM in the presence and absence of exendin (9–39) (Ex; 100 nM) ($n = 4$/group). * indicates $p < 0.05$ compared to saline or blank SSM-treated cells. # indicates $p < 0.05$ compared to respective GLP-1 in saline or GLP1-SSM. **b** Fold increase in culture media insulin concentration of RINm5F cells incubated with GLP-1 (10 nM) in saline or GLP1-SSM, relative to respective saline or blank SSM controls. * indicates $p < 0.05$ compared to saline or blank SSM treated control cells ($n = 3$/group).

246.1 ± 29.2 pg/ml; TNF-α, 113.4 ± 32.8 pg/ml) or GLP-1 in saline (IL-6, 227.7 ± 38.1 pg/ml; TNF-α, 123.2 ± 12.2 pg/ml) treatments (each, $p < 0.05$ compared to GLP1-SSM, $n = 6$/group). To confirm these observed results were due to direct anti-inflammatory effects of GLP1-SSM on the inflamed lungs in ALI mice, the liver tissue MPO activity was measured to detect presence of systemic inflammation. Our data revealed similar MPO activity between LPS-nebulized ALI mice and baseline control mice (Supplementary Fig S1).

In Vivo **Anti-inflammatory Dose Response Effects of GLP1-SSM**

Increasing the dose of GLP1-SSM from 5–30 nmol/mouse resulted in a dose-dependent decrease in the BALF neutrophil
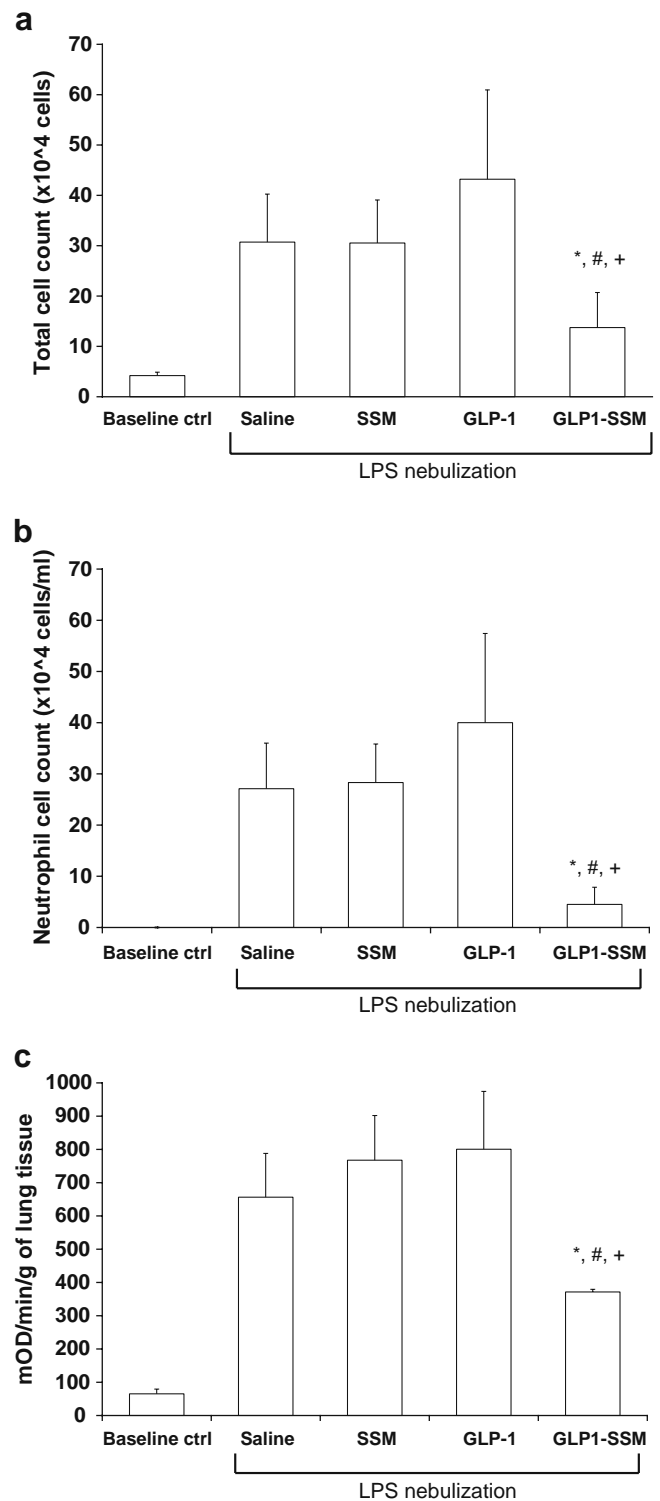

a

b

c

Fig. 3 Effects of GLP1-SSM against neutrophilic influx into lungs of ALI mice. **a-b** Total cell count **a** and neutrophil cell count **b** in BALF of ALI mice. **c** Myeloperoxidase (MPO; mOD/min/g of tissue) assay activity of ALI mice lung tissues. LPS-induced ALI mice were treated with saline, SSM, GLP-1 in saline (GLP-1; 15 nmol/mouse) or GLP1-SSM. *, # and + indicate $p < 0.05$ compared to saline, SSM and GLP-1 treatments respectively ($n = 6$/group).
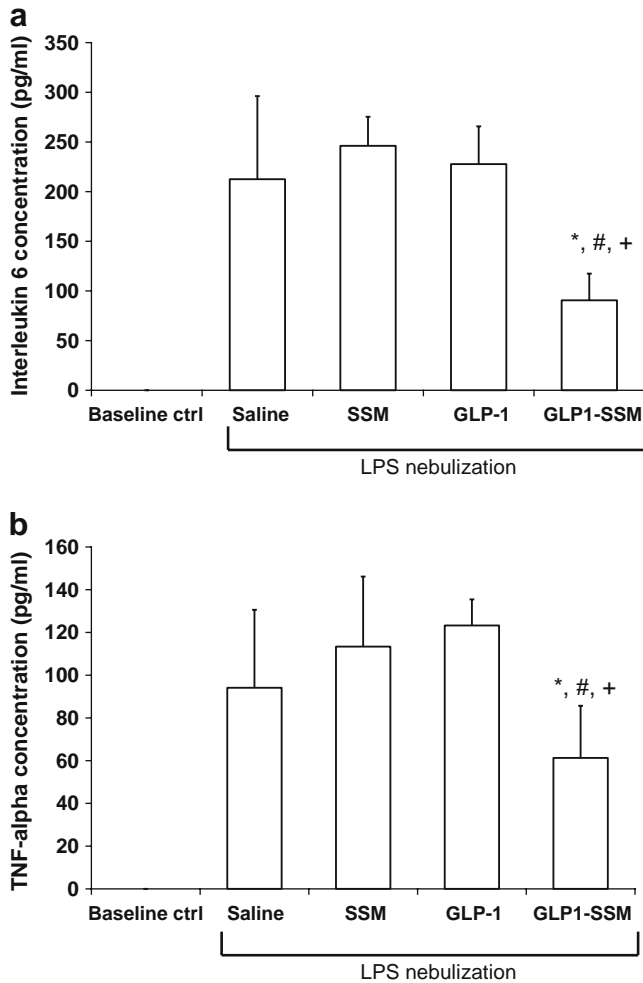
Fig. 4 Effects of GLP1-SSM against pro-inflammatory cytokine production in lungs of ALI mice. **a-b**, IL- 6 **a** and TNF-α **b** concentrations in BALF of ALI mice. LPS-induced ALI mice were treated with saline, SSM, GLP-1 in saline (GLP-1; 15 nmol/mouse) or GLP1-SSM. *, # and + indicate $p <$ 0.05 compared to saline, SSM and GLP-1 treatments, respectively ($n = 6$/group).

cell count in ALI mice (5 nmol, $14.0 \pm 8.4 \times 10^4$ cells/ml; 15 nmol, $4.5 \pm 3.4 \times 10^4$ cells/ml; 30 nmol, $2.0 \pm 1.7 \times 10^4$ cells/ml) (Fig. 5a). Similarly, significantly lower MPO activity was measured in the murine lung tissue with an increasing dose of GLP1-SSM (5 nmol, 423.7 ± 37.6 mOD/min/g of tissue; 15 nmol, 371.3 ± 7.9 mOD/min/g of tissue; 30 nmol, 327.6 ± 27.8 mOD/min/g of tissue) (Fig. 5b). Even though there was no statistical significance among the BALF IL-6 concentration measured at increasing peptide dose, a similar decreasing trend was observed (Fig. 5c). These *in vivo* anti-inflammatory effects of s.c. GLP1-SSM (5–30 nmol/mouse) were also comparable to those of s.c. methylprednisolone (3 mg/kg), a common drug used for the treatment of clinical ALI, in the same animal model (Fig. 5a-c).

DISCUSSION

Human GLP-1 Spontaneously Associates to SSM

Based on the data obtained by CD spectroscopy, GLP-1 exhibited significant α-helical structure when added to SSM dispersion. This is in stark contrast to samples of GLP-1 in saline where random coil conformation was demonstrated
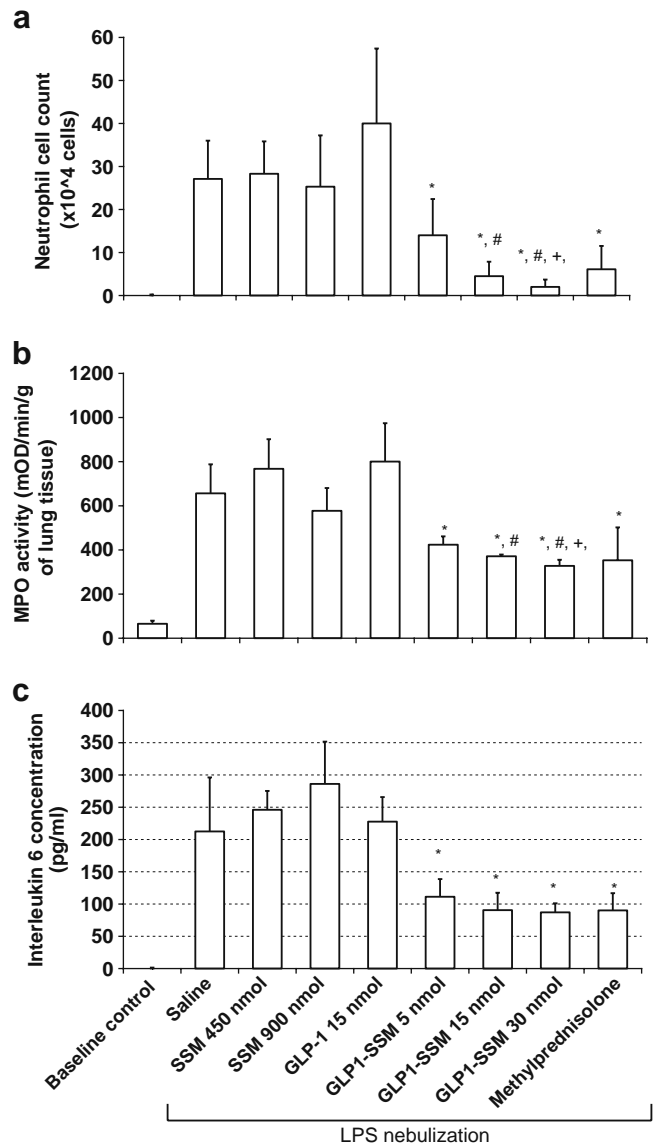

Fig. 5 Dose response anti-inflammatory effects of GLP1-SSM in comparison to methylprednisolone. **a-c** BALF neutrophil cell count **a** lung tissue MPO (mOD/min/g of tissue) assay activity **b** and BALF IL-6 concentration **c** in ALI mice at increasing peptide dose of s.c. GLP1-SSM (5–30 nmol/mouse) or methylprednisolone (3 mg/kg). * indicates $p < 0.05$ compared to saline, SSM and GLP-1 treatment groups. #, + indicate $p < 0.05$ compared to GLP1-SSM 5 nmol and GLP1-SSM 15 nmol respectively ($n = 6$/group).

(Fig. 1a). Correspondingly, the micron-sized peptide aggregates in saline (1721.9 ± 1285.1 nm; $n=3$) were also eliminated when GLP-1 was added to SSM dispersion, giving a reproducible single size peak at 13.6 ± 3.1 nm (particle size of SSM) (Fig. 1b). These results implied spontaneous interaction of GLP-1 with SSM in saline (aqueous medium) to undergo a secondary conformational change in the associated peptide molecule to display increased α-helicity, which is the preferred conformation for receptor interaction. Fluorescence spectroscopy analysis of GLP-1 (5 μM) in SSM demonstrated a lipid: peptide saturation molar ratio of 13:1 (Fig. 1c), which translated to a loading capacity of approximately six GLP-1 molecules for each SSM at saturation [17].

For an amphipathic peptide such as GLP-1, it is generally postulated that its micelle association is governed, most likely, by electrostatic and hydrophobic driving forces between the respective charge and hydrophobic amino acid moieties of the peptide and micelle in aqueous media [24–26]. Correspondingly, when GLP1-SSM comes within close proximity of the peptide-specific receptor, the greater attractive interaction(s) between the ligand and specific receptor cause the release of GLP-1 from SSM to allow interaction with its specific receptor.

Of note, preparation of GLP1-SSM dispersion is simple and therefore possibly reproducible at large scale [13]. The resulting formulation can also be sterilized by sterile filtration (Supplementary Material Fig. S2) and freeze-dried without additional cryo- or lyo-protectants [13]. This sterilized freeze-dried product can potentially allow longer shelf storage in the dried state and be reconstituted in water for injection just before use in patients. Collectively, these data indicated that a novel nanomedicine of GLP-1 that can be easily translated to the clinics is developed.

Human GLP-1 Binds and Activates GLP-1R *In Vitro* When Associated with SSM

To investigate the bioactivity of GLP-1 when associated with SSM, we determined the ability of GLP1-SSM to bind and activate GLP-1R *in vitro* through quantification of its downstream secondary messenger, cAMP, and secretory product, insulin. GLP1-SSM (10 nM GLP-1) induced similar increase in cAMP concentration compared to GLP-1 in saline (Fig. 2a). GLP-1R specificity for this observed effect was demonstrated by the attenuation response produced by co-administration of GLP-1R antagonist, exendin (9–39) (Ex, 100 nM). Likewise, similar increment in culture media insulin concentration was measured when RINm5F cells were incubated with GLP1-SSM (10 nM GLP-1) or GLP-1 in saline, relative to saline/blank SSM-treated control cells (Fig. 2b). Since serum-free or serum-reduced media were used in these *in vitro* studies, the absence/reduced

concentration of serum enzymes could probably explain the lack of activity loss with GLP-1 in saline, due to less enzyme-induced peptide degradation in this cell culture system. Overall, the cell culture data showed that GLP1-SSM was able to bind and activate GLP-1R at the same rate as free GLP-1 in saline. Since the anti-inflammatory effect of GLP-1 (in aqueous media) was enacted through GLP-1R [6], these *in vitro* results clearly indicated that the anti-inflammatory activity of GLP-1 is retained when associated with SSM.

GLP1-SSM Suppresses Lung Inflammation in LPS-Induced ALI Mice

To study the anti-inflammatory activity of GLP1-SSM against acute lung injury, the test formulation was administered s.c. to mice with ALI induced via nebulization of LPS solution. LPS nebulization allows the development of isolated ALI while eliminating possible complications that may arise as a result of multiple organ failures with parenteral LPS [20,21,27]. The resulting lung inflammatory responses, induced by a single episode of nebulized LPS, were highly reproducible and showed comparable magnitude relative to mice given single i.p. injection of low dose LPS (3 mg/kg) [22].

Neutrophil accumulation and activation in lungs have been frequently cited as major symptoms responsible for propagation of lung inflammation in ALI [28]. This characteristic phenomenon was also observed in our chosen model of ALI mice (Fig. 3a and b). Evidence of s.c. GLP1-SSM (15 nmol of GLP-1/mouse) anti-inflammatory effects against LPS-induced lung hyper-inflammation were apparent by the observed suppression in BALF total and neutrophil cell count, and MPO activity in treated ALI mice (Fig. 3a-c). Based on these results, the ability of GLP1-SSM to suppress neutrophil accumulation and/or activation in lungs may hence be an important mechanism for its anti-inflammatory response. According to published literature, potential mechanisms of cAMP elevation on suppression of neutrophil transendothelial migration and chemotaxis in an inflammation event include [29–31] 1) inhibition of neutrophil cell rolling in circulation, postulated to be mediated through downregulation of E-selectin expressed on endothelial cells and secondary nitric oxide release, 2) inhibition of cellular actin polymerization, which is responsible for the changes in neutrophil deformability required to extend its capillary transit time and increase concentration of neutrophil at an inflammation site, 3) decreased chemotactic responsiveness of neutrophil to chemoattractants released during inflammation. On the basis that GLP-1R activation induced cAMP production (Fig. 2a and Supplementary Material Fig. S3), the observed suppression in

neutrophilic influx into the lungs of ALI mice given GLP1-SSM could therefore be potentially due to GLP-1R activation by GLP-1 delivered in SSM.

Besides neutrophil, IL-6 and TNF-α are common pro-inflammatory cytokines typically upregulated in ALI (20,32). LPS-induced lung hyper-inflammation brought about increased IL-6 (Fig. 4a) and TNF-α (Fig. 4b) concentrations in BALF of ALI mice that were similarly suppressed by GLP1-SSM administration (IL-6, 90.5 ± 26.9 pg/ml; TNF-α, 61.3 ± 24.4 pg/ml). Since there was no detectable elevation in the liver tissue MPO activity of ALI mice compared to baseline controls (Supplementary Material Fig. S1), generalized systemic inflammation was deduced to be minimal and insignificant. The anti-inflammatory effects of GLP1-SSM were thus attributed to its direct activities in the inflamed murine lung tissues. For all these inflammatory parameters studied, no significant downregulation was seen in mice receiving GLP-1 in saline at the same dose. These data illustrate the importance of delivering GLP-1 in SSM for *in vivo* anti-inflammatory efficacy by protecting the peptide from enzymatic degradation and most probably targeting it by EPR effects to the sites of inflammation.

GLP1-SSM Suppresses Lung Inflammation in a Dose-Dependent Fashion

To evaluate dose response effect of GLP1-SSM, increasing peptide doses (5, 15 or 30 nmol of GLP-1/mouse) were administered s.c. to ALI mice. Our data showed apparent dose response effects for GLP1-SSM within the peptide dose range studied (Fig. 5a-c), with enhanced anti-inflammatory activity at higher peptide dose of GLP1-SSM. Furthermore, since the observed anti-inflammatory response did not reach plateau within the tested dose range (Fig. 5a), further increase in anti-inflammatory activity is still possible at higher peptide dose of GLP1-SSM. Lastly, these anti-inflammatory effects of GLP1-SSM (5–30 nmol/mouse) were observed to be comparable to those of s.c. methyl-prednisolone (3 mg/kg) in the same animal model, attesting to the potency of GLP1-SSM *in vivo* (Fig. 5a-c).

Previous studies of blank SSM administered subcutaneously at 0.2 mmol/kg (which is approximately 5 µmol/mouse) to collagen-induced arthritic mice did not reveal any detectable toxicity with regards to their serum chemistry and hematological parameters (33). Therefore, given that the doses of lipid used for these ALI animal studies were much lower (0.9 µmol/mouse or below), we do not anticipate any significant toxicity to be observed due to SSM. Likewise, clinical use of GLP-1 (8 ng/kg/min of i.v. infusion over 24 h which translated to 3 nmol/kg) has only highlighted nausea and vomiting as its significant common side effects (34,35). Even though the anti-inflammatory doses of GLP-1 (0.2–

1.2 µmol/kg in mouse) used in this study are higher, we have not observed any different behavior or appearance for the treated mice compared to the control mice. This may be due to the fact that GLP-1 was associated with SSM during circulation and released predominantly at the inflammation sites, thereby minimizing non-specific side effects. Therefore, it is highly promising that our proposed GLP1-SSM formulation will be an effective and safe nanomedicine for the treatment of ALI.

CONCLUSIONS

Taken together, these results indicate that human GLP-1 self-associated with PEGylated phospholipid micelles (GLP1-SSM) to form a promising novel, anti-inflammatory nanomedicine for the treatment of Gram-negative sepsis-induced ALI/ARDS. *In vivo* administration of GLP1-SSM to LPS-induced ALI mice resulted in significant downregulation of lung inflammation, with dose-dependent anti-inflammatory activity observed. Since similar therapeutic activity had not been detected for GLP-1 in saline, the SSM nanocarriers therefore played a critical role in protecting the enzyme-labile GLP-1 and delivering it to inflamed tissues *in vivo*. In summary, this study demonstrated for the first time that the developed novel lipid-based formulation of GLP-1 is effective against ALI and can be easily translated to the clinics to treat this important disease. In addition, given that GLP-1 is an established glucose-lowering agent (34) and hyperglycemia is a common complication in septic patients known to aggravate the progression of sepsis-induced ALI (36–38), GLP1-SSM is likely to function as a glucose-regulating agent as well in sepsis-induced ALI to show dual function to modulate lung hyper-inflammation.

REFERENCES

1. Angus DC, Clermont G, Linde-Zwirble WT, Musthafa AA, Dremsizov TT, Lidicker J, *et al.* Healthcare costs and long-term

outcomes after acute respiratory distress syndrome: A phase III trial of inhaled nitric oxide. Crit Care Med. 2006;34(12):2883–90.

2. Rubenfeld GD, Herridge MS. Epidemiology and outcomes of acute lung injury. Chest. 2007;131(2):554–62.

3. Bosma KJ, Lewis JF. Emerging therapies for treatment of acute lung injury and acute respiratory distress syndrome. Expert Opin Emerg Drugs. 2007;12(3):461–77.

4. Holst JJ. The physiology of glucagon-like peptide 1. Physiol Rev. 2007;87(4):1409–39.

5. Blandino-Rosano M, Perez-Arana G, Mellado-Gil JM, Segundo C, Aguilar-Diosdado M. Anti-proliferative effect of pro-inflammatory cytokines in cultured beta cells is associated with extracellular signal-regulated kinase 1/2 pathway inhibition: protective role of glucagon-like peptide -1. J Mol Endocrinol. 2008;41(1):35–44.

6. Iwai T, Ito S, Tanimitsu K, Udagawa S, Oka J. Glucagon-like peptide-1 inhibits LPS-induced IL-1beta production in cultured rat astrocytes. Neurosci Res. 2006;55(4):352–60.

7. Baggio LL, Drucker DJ. Biology of incretins: GLP-1 and GIP. Gastroenterology. 2007;132(6):2131–57.

8. Lee KC, Chae SY, Kim TH, Lee S, Lee ES, Youn YS. Intrapulmonary potential of polyethylene glycol-modified glucagon-like peptide-1s as a type 2 anti-diabetic agent. Regul Pept. 2009;152(1–3):101–7.

9. Yin D, Lu Y, Zhang H, Zhang G, Zou H, Sun D, *et al.* Preparation of glucagon-like peptide-1 loaded PLGA microspheres: characterizations, release studies and bioactivities *in vitro/in vivo*. Chem Pharm Bull. 2008;56(2):156–61.

10. Weise WJ, Sivanandy MS, Block CA, Comi RJ. Exenatide-associated ischemic renal failure. Diab Care. 2009;32(2):e22–3.

11. Philippe J, Raccah D. Treating type 2 diabetes: how safe are current therapeutic agents? Int J Clin Pract. 2009;63(2):321–32.

12. Ashok B, Arleth L, Hjelm RP, Rubinstein I, Onyuksel H. *In vitro* characterization of PEGylated phospholipid micelles for improved drug solubilization: effects of PEG chain length and PC incorporation. J Pharm Sci. 2004;93(10):2476–87.

13. Lim SB, Rubinstein I, Onyuksel H. Freeze drying of peptide drugs self-associated with long-circulating, biocompatible and biodegradable sterically stabilized phospholipid nanomicelles. Int J Pharm. 2008;356(1–2):345–50.

14. Sethi V, Onyuksel H, Rubinstein I. Enhanced circulation half-life and reduced clearance of vasoactive intestinal peptide (VIP) loaded in sterically stabilized phospholipid micelles (SSM) in mice with collagen-induced arthritis (CIA). AAPS PharmSci. 2003;5 Suppl 1:M1045.

15. Koo OM, Rubinstein I, Onyuksel H. Role of nanotechnology in targeted drug delivery and imaging: a concise review. Nanomedicine. 2005;1(3):193–212.

16. Sadikot RT, Rubinstein I. Long-acting, multi-targeted nanomedicine: addressing unmet medical need in acute lung injury. J Biomed Nanotechnol. 2009;5(6):614–9.

17. Arleth L, Ashok B, Onyuksel H, Thiyagarajan P, Jacob J, Hjelm RP. Detailed structure of hairy mixed micelles formed by phosphatidylcholine and PEGylated phospholipids in aqueous media. Langmuir. 2005;21(8):3279–90.

18. Stark A, Mentlein R. Somatostatin inhibits glucagon-like peptide-1-induced insulin secretion and proliferation of RINm5F insulinoma cells. Regul Pept. 2002;108(2–3):97–102.

19. John H, Maronde E, Forssmann WG, Meyer M, Adermann K. N-terminal acetylation protects glucagon-like peptide GLP-1-(7–34)-amide from DPP-IV-mediated degradation retaining cAMP- and insulin-releasing capacity. Eur J Med Res. 2008;13(2):73–8.

20. Ingenito EP, Mora R, Cullivan M, Marzan Y, Haley K, Mark L, *et al.* Decreased surfactant protein-B expression and surfactant dysfunction in a murine model of acute lung injury. Am J Respir Cell Mol Biol. 2001;25(1):35–44.

21. Baron RM, Carvajal IM, Fredenburgh LE, Liu X, Porrata Y, Cullivan ML, *et al.* Nitric oxide synthase-2 down-regulates surfactant protein-B expression and enhances endotoxin-induced lung injury in mice. FASEB J. 2004;18(11):1276–8.

22. Yull FE, Han W, Jansen ED, Everhart MB, Sadikot RT, Christman JW, *et al.* Bioluminescent detection of endotoxin effects on HIV-1 LTR-driven transcription *in vivo*. J Histochem Cytochem. 2003;51(6):741–9.

23. Jeyaseelan S, Chu HW, Young SK, Worthen GS. Transcriptional profiling of lipopolysaccharide-induced acute lung injury. Infect Immun. 2004;72(12):7247–56.

24. Krishnadas A, Onyuksel H, Rubinstein I. Interactions of VIP, secretin and PACAP(1–38) with phospholipids: a biological paradox revisited. Curr Pharm Des. 2003;9(12):1005–12.

25. Bourbigot S, Dodd E, Horwood C, Cumby N, Fardy L, Welch WH, *et al.* Antimicrobial peptide RP-1 structure and interactions with anionic *versus* zwitterionic micelles. Biopolymers. 2009;91 (1):1–13.

26. Tinoco LW, Gomes-Neto F, Valente AP, Almeida FC. Effect of micelle interface on the binding of anticoccidial PW2 peptide. J Biomol NMR. 2007;39(4):315–22.

27. Sadikot RT, Jansen ED, Blackwell TR, Zoia O, Yull F, Christman JW, *et al.* High-dose dexamethasone accentuates nuclear factor-kappa b activation in endotoxin-treated mice. Am J Respir Crit Care Med. 2001;164(5):873–8.

28. Bream-Rouwenhorst HR, Beltz EA, Ross MB, Moores KG. Recent developments in the management of acute respiratory distress syndrome in adults. Am J Health Syst Pharm. 2008;65(1):29–36.

29. Sato Y. Modulation of PMN-endothelial cells interactions by cyclic nucleotides. Curr Pharm Des. 2004;10(2):163–70.

30. Stephens CG, Snyderman R. Cyclic nucleotides regulate the morphologic alterations required for chemotaxis in monocytes. J Immunol. 1982;128(3):1192–7.

31. Harvath L, Robbins JD, Russell AA, Seamon KB. cAMP and human neutrophil chemotaxis. Elevation of cAMP differentially affects chemotactic responsiveness. J Immunol. 1991;146(1):224–32.

32. Tsushima K, King LS, Aggarwal NR, De Gorordo A, D'Alessio FR, Kubo K. Acute lung injury review. Intern Med. 2009;48 (9):621–30.

33. Koo OM. A novel nanomedicine against arthritis: targeted camptothecin phospholipid micelles. PhD Thesis, University of Illinois at Chicago; 2006.

34. Drucker DJ, Nauck MA. The incretin system: glucagon-like peptide-1 receptor agonists and dipeptidyl peptidase-4 inhibitors in type 2 diabetes. Lancet. 2006;368(9548):1696–705.

35. Larsen J, Hylleberg B, Ng K, Damsbo P. Glucagon-like peptide-1 infusion must be maintained for 24 h/day to obtain acceptable glycemia in type 2 diabetic patients who are poorly controlled on sulphonylurea treatment. Diab Care. 2001;24(8):1416–21.

36. Chen HI, Yeh DY, Liou HL, Kao SJ. Insulin attenuates endotoxin-induced acute lung injury in conscious rats. Crit Care Med. 2006;34(3):758–64.

37. Hagiwara S, Iwasaka H, Hasegawa A, Koga H, Noguchi T. Effects of hyperglycemia and insulin therapy on high mobility group box 1 in endotoxin-induced acute lung injury in a rat model. Crit Care Med. 2008;36(8):2407–13.

38. Cohen J. The immunopathogenesis of sepsis. Nature. 2002;420 (6917):885–91.